CONFTELE '99 ISBN 972-98115-0-4
Proc. CONFTELE 1999 - II Conf. de Telecomunicações, Sesimbra, Portugal, 466-470, Abr 1999

Co-Siting Criteria for Wind Turbine Generators and Transmitter Antennas

Carlos Salema, Carlos Fernandes
Instituto Superior Técnico and Instituto de Telecomunicações, Lisboa, Portugal

Abstract—**Transmitter antennas, for VHF and higher frequencies, are usually installed in hill-tops and mountain-tops to improve coverage. These sites tend to be windy and thus are favorable locations for wind turbine generators, particularly if alone or in very small wind farms. Modern wind turbine generators make use of large solid metallic pylons which, if located too close to the antennas, will cause severe modifications to the antenna radiation pattern and thus to the quality of service. Using WIPL-D we have modeled a typical antenna and a wind turbine at 100 MHz in order to provide criteria for co-siting. The increase in the number of unknowns with increasing operating frequency prevented the analysis to be extended to the GSM band – 900 MHz –. An alternative formulation based on the Kirchhoff-Huygens vector formulas was used to cover from 100 MHz to 1000 MHz, enabling both to confirm the previous results and to extend them.**

Keywords—**wind turbine generator, WIPL-D, cellular radio**

I. Introduction

Transmitter antennas, for VHF and higher frequencies, are usually installed in isolated hill-tops and mountain-tops to improve coverage. Favorable sites are often rather crowded but mutual interference is kept to acceptably low levels due to one or more of the following factors: tower siting, distance between towers, small tower cross-section and high antenna directivity.

Good antenna sites tend to be windy and thus are favorable locations for wind turbine generators, particularly if alone or in very small wind farms. However modern wind turbine generators employ large solid metallic pylons which have a much larger cross-section and thus will cause severe blockage to the antenna radiation pattern and to the quality of service if located too close to the antennas.

This problem arises mostly at frequencies between 100 MHz and 1000 MHz used both for radio and TV broadcasting and for mobile (cellular) radio. In any case the presence of the wind turbine generator is felt as a modification of the signal intensity on the area of coverage which becomes objectionable if perceived by the user. There seems to be preciously little published data on this subject from which design criteria might be derived.

For analog transmission (FM radio and TV) average user awareness threshold varies with the intensity of the received signal but may roughly be stated as being about ± 3 dB, except very close to the transmitter, when the received signal is likely to saturate the receiver. In the latter case a larger received signal decrease (possibly up to - 6 dB) may well be acceptable.

For digital transmission, such as used in GSM cellular radio, the situation is quite different. The bit error rate increases as the received signal decreases but, up to a minimum signal level, the user is likely to be unaware of the fact. In this case the criteria for co-sitting should be the minimum signal level, rather than a change in the signal level due to the presence of the wind turbine generator. To further complicate matters radio cell radius may vary from less than 1 km up to about 25 km (according to the expected traffic) and cells often overlap so that if the signal from a transmitter falls below the threshold level the service may be guaranteed by another transmitter.

Since wind turbine generators are always located in fairly isolated places we may reasonably assume that cell radius would be large, from 10 to 20 km, and with little or no overlapping.

II. Modeling using WIPL-D

We assumed the wind turbine generator to be made up of a solid cylindric pylon (perfect conductor), 3 m in diameter and 40 m high, with 3 (loss-less) dielectric blades, each 20 m long and 1 m wide. The transmitter antenna was taken as a half wavelength dipole mounted at a distance d_t from the axis of the pylon and at a height of 30 m, and the receiver antenna was a short dipole at the height of 1.5 m. Due to the distances involved (up to 20 km) Earth curvature was neglected.

We started by modeling the transmitter antenna and the wind turbine generator, shown in figure 1, using WIPL-D [1], [2]. Even if this program provided a very good model, up to the inclusion of the blades, it becomes unusable when trying to extend the analysis up to 1000 MHz due to the large number of unknowns involved.

Disregarding ground effects, the far field radiation pattern of the transmitter antenna in the horizontal plane is constant, with a directivity of 2.16 dB. The presence of the wind turbine generator introduces perturbations in this pattern at 100 MHz as shown in figures 2, 3 and 4, for a transmitter antenna height of 30 m and distances to the pylon axis d_t equal to 50 m, 100 m and 200 m respectively.

From these figures we confirm that, as expected, the influence of the wind generator turbine in the transmitter antenna radiation pattern decreases as the distance d_t increases. For distances greater than about 50 m the presence of the wind turbine generator is not likely to be felt by most radio listeners and VHF TV viewers.

The height of the transmitter antenna does not have a significant impact on the results (compare figures 5 and 3) except when it becomes higher than the wind turbine

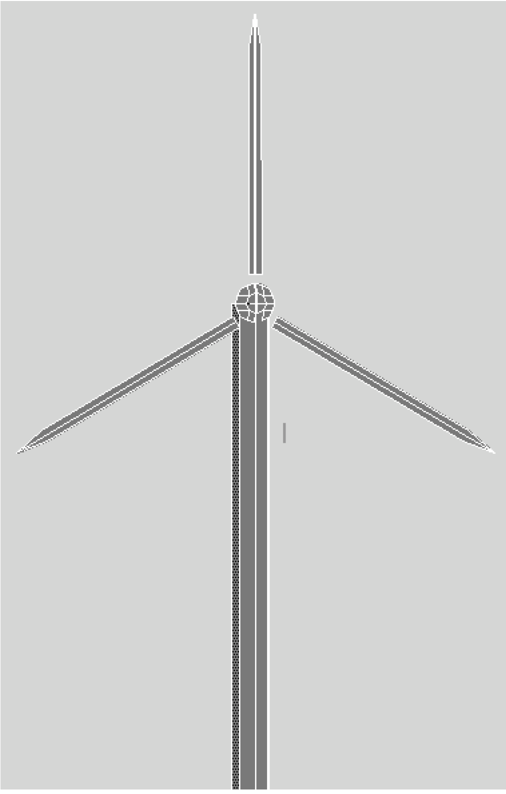

Fig. 1. Schematic representation of the wind turbine generator as simulated using WIPL-D.

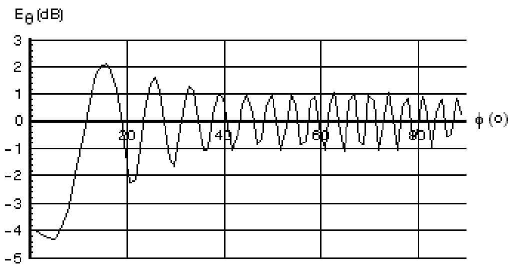

Fig. 2. Far field radiation pattern for a pylon axis distance of 50 m at 100 MHz.

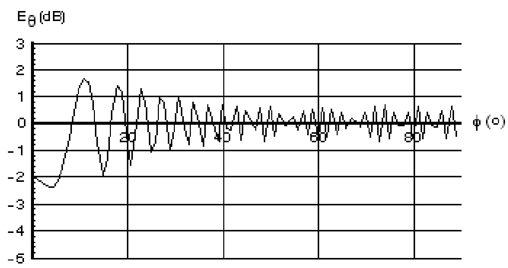

Fig. 3. Far field radiation pattern for a pylon axis distance of 100 m at 100 MHz.

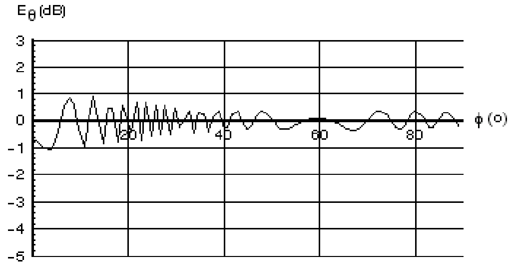

Fig. 4. Far field radiation pattern for a pylon axis distance of 200 m at 100 MHz.

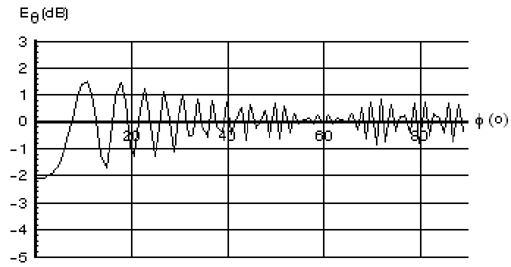

Fig. 5. Far field radiation pattern for a transmitter antenna height of 20 m and a distance of 100 m to the pylon axis at 100 MHz.

pylon in which case the disturbance decreases very rapidly (figures 3 and 6).

Static blades, even when assumed to be metallic, have very little influence in the results.

It is instructive to plot the excess obstacle attenuation close to the pylon. Figure 7, shows the obstacle attenuation for $d_t = 200$ m and a transmitter antenna height of 30 m at 100 MHz, where the darker areas correspond to the higher attenuation. The dynamic range is rather small, between -3.4 and $+2.3$ dB. Negative values of attenuation imply that field intensities are below their free-space value.

For higher frequencies, typical of cellular radio, WIPL-D quickly becomes impractical due to the increase in the number of unknowns. An alternative method must thus be used.

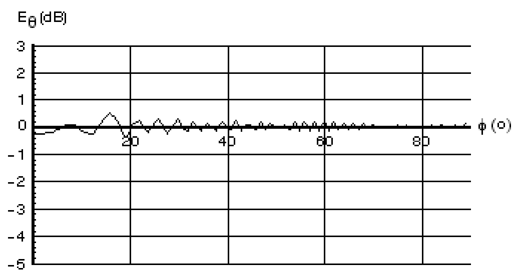

Fig. 6. Far field radiation pattern for a transmitter antenna height of 50 m and a distance of 100 m to the pylon axis at 100 Mhz.

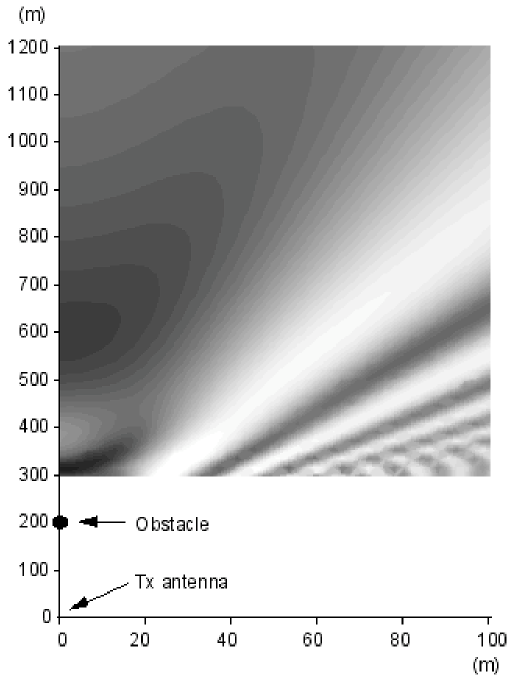

Fig. 7. Obstacle attenuation for $d = 200$ m calculated using WIPL-D at 100 MHz.

III. Modeling with a finite width plate

In radio link design it is common practice to replace obstacles by equivalent knife-edges. This approach provided good results at large distances from the obstacle, where its attenuation is reasonably independent from obstacle shape according to obstacle theory.

Since finite cylindrical obstacles are notoriously hard to deal with, we replace the pylon by a rectangular plate with an area equal to the cylinder cross-section. Under these conditions the classical Kirchhoff-Huygens formulation can be used to derive the excess attenuation A in dB caused by a rectangular opaque plate:

$$A = 10 \log_{10} \left(\frac{a}{4} \right) \tag{1}$$

with:

$$\begin{aligned} a = \Big\{ [C(w_2) \; &- \; C(w_1)] \left[C(h_e) - \frac{1}{2} \right] - \\ [S(w_2) \; &- \; S(w_1)] \left[S(h_e) - \frac{1}{2} \right] \Big\}^2 + \\ \Big\{ 2 + [S(w_2) \; &- \; S(w_1)] \left[C(h_e) - \frac{1}{2} \right] + \\ [C(w_2) \; &- \; C(w_1)] \left[S(h_e) - \frac{1}{2} \right] \Big\}^2 \end{aligned} \tag{2}$$

where:

$$c = \sqrt{\pi d_t d_r (d_t + d_r)} \tag{3}$$

$$h_e = \frac{x_r d_t + x_t d_r}{c} \tag{4}$$

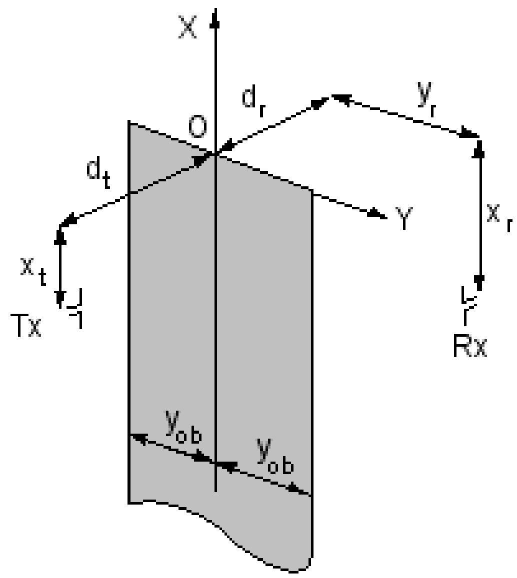

Fig. 8. Finite width plate geometry.

$$w_1 = \frac{(d_t + d_r) y_{ob} - y_r d_t}{c} \tag{5}$$

$$w_2 = \frac{(d_t + d_r) y_{ob} + y_r d_t}{c} \tag{6}$$

and d_r, d_t, x_r, x_t, y_t and y_{ob} are obtained from figure 8 after normalization, that is, multiplication by $\frac{2\pi}{\lambda}$ where λ is the free-space wavelength. $C(x)$ and $S(x)$ are the Fresnel integrals defined in [3].

Figure 9 shows the obstacle attenuation calculated using 2 for the same conditions as before. Diffraction effects at the sharp edges of the finite width knife-edge are expected to underestimate the attenuation for certain regions but comparison with cylinder obstacle results from WIPL-D at 100 MHz shows that the differences are not significant (Figures 7 and 9), that is usually under about 1 dB, particularly in the shadow region. A closer examination of the results shows that the maximum and minimum values of attenuation in both methods are mostly within ± 0.5 dB, although their location may be slightly displaced. We expect the finite width knife-edge to become more accurate as the frequency increases.

Using the finite plate approximation we have also calculated the effect of the obstacle in the far field radiation pattern of the transmitter antenna for d_t in the range 50 to 200 m. The results match very closely, well within ± 0.5 dB, those obtained using WIPL-D, particularly in the shadow region. The only exception is when the distance between the obstacle and the transmitter antenna falls below about 75 m, where differences between the two methods may reach about 1.5 dB.

Once the rectangular plate approximation has been established we can now proceed to calculate the obstacle attenuation for 1000 MHz ($\lambda = 0.3$ m). Figure 10 shows the results for a pylon 200 m away from the transmitter antenna. Now the shadow is better defined and the

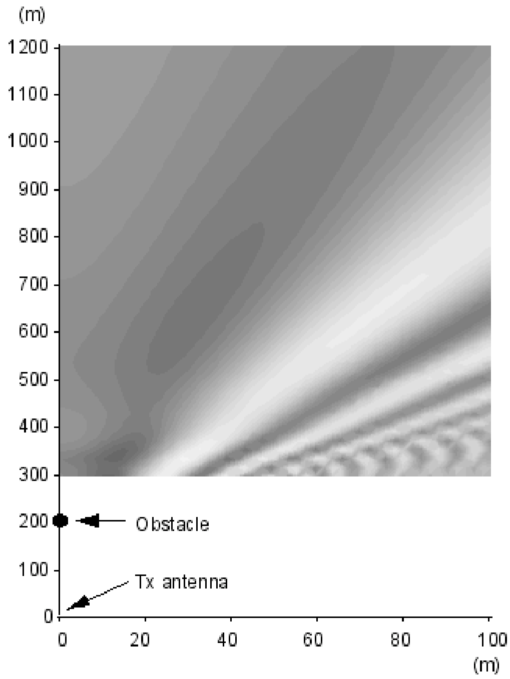

Fig. 9. Obstacle attenuation for $d = 200$ m calculated using the Kirchhoff-Huygens formulation at 100 MHz.

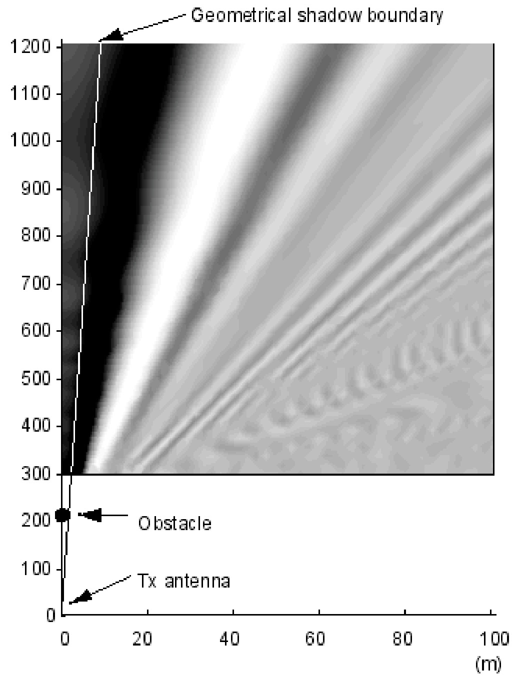

Fig. 10. Obstacle attenuation for $d = 200$ m calculated using the Kirchhoff-Huygens formulation.

attenuation is higher than before (−6.4 dB) just behind the pylon. As expected the higher attenuation region approaches the geometrical shadow region.

For smaller distances between the obstacle and the transmitter antenna, the width of the shadow region and the attenuation within it both increase. The latter behaviour is displayed in Figure 11 which represents the maximum attenuation in the same 100 m by 900 m region as before, calculated using the finite width plate for different values of d_t and frequencies of 100 and 1000 MHz.

Figure 11 shows that pylon attenuation is not significant at 100 MHz since the calculated worst case values are not likely to affect typical applications at this frequency. A different conclusion is obtained at 1000 MHz. Now, the influence of the obstacle cannot be neglected even for a transmitter antenna to pylon distance as large as 200 m. However worst case values correspond to rather small areas (tens of metres across) in the shadow region, which may be acceptable for cellular radio planning.

The effect of the obstacle in the far field radiation pattern of the transmitter antenna is clearly more pronounced at 1000 MHz than at 100 MHz. Figure 12 shows the far field radiation pattern at 1000 MHz for d_t equal to 50, 100 and 200 m. Now for the lower distances ($d_t = 50$ m) the effect on the transmitter antenna radiation pattern is likely to affect the quality of service in a rather narrow region, corresponding to the geometrical shadow region (≈ 1.7 degrees).

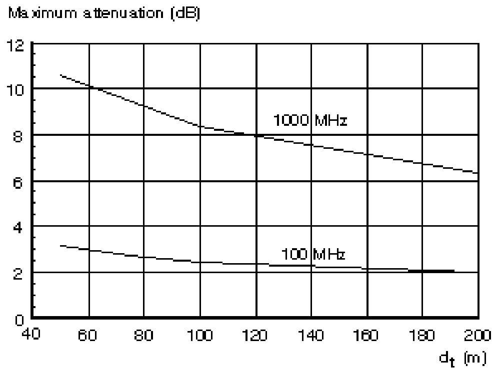

Fig. 11. Maximum attenuation as a function of transmitter antenna to obstacle distance d_t.

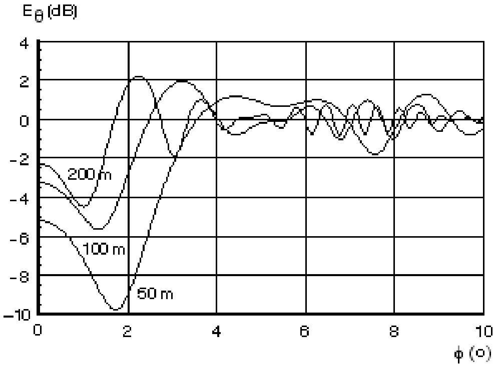

Fig. 12. Far field radiation pattern for transmitter antenna to pylon axis distances of 50, 100 and 200 m, at 100 MHz.

IV. Discussion

From the results presented for a single obstacle we may derive the following tentative rules-of-thumb for co-siting of transmitter antennas and wind turbine generators:

• For frequencies around 100 MHz, the minimum distance between the transmitter antenna and the pylon of the wind turbine generator should not be less than about 50 m in most cases, unless the transmitter antenna is placed considerably higher than the top of the pylon. Increasing this distance to 100 m decreases the perturbations which are unlikely to be felt except very close to the wind turbine generator.

• For frequencies around 1000 MHz, the minimum distance between the transmitter antenna and the pylon of the wind turbine generator has to increase considerably, from 50 to 100 or preferably 200 m, the shorter distances (around 50 m) displaying a significant dip in the radiation pattern, closely corresponding to the geometrical shadow region.

• For frequencies above 1000 MHz the shadowing effect of the pylon will increase and thus even larger distances become necessary.

The results presented in this paper refer to a single obstacle. Simulations using WIPL-D for combinations of two similar obstacles show that the excess attenuation is only slightly higher in the immediate vicinity (less than 100 m) of the obstacles, within its geometrical shadow region. It is thus expected that attenuation caused by wind farms may be calculated using models for isolated wind generators.

All the discussion refers to the diffraction effect of the obstacle, which is expected to be the main phenomena in typical cases. However, when either the base station antenna or the mobile antenna are well above the obstacle tip, reflections on the turning blades may also affect the received signal. These were not considered here.

References

[1] B. Kolundzija and B. Reljic, “Plate modeling of wire structures,” *Proceedings of the IEEE APS International Symposium*, vol. 3, pp. 1798–1801, 1997.

[2] B. Kolundzija, “Electomagnetic modeling of composite metallic and dielectric structures,” *Proceedings of the IEEE APS International Symposium*, vol. 3, pp. 1822–1825, 1997.

[3] M. Abramowitz and I. Stegun, *Handbook of Mathematical Functions*, Dover Publications, Inc., New York, 1968.